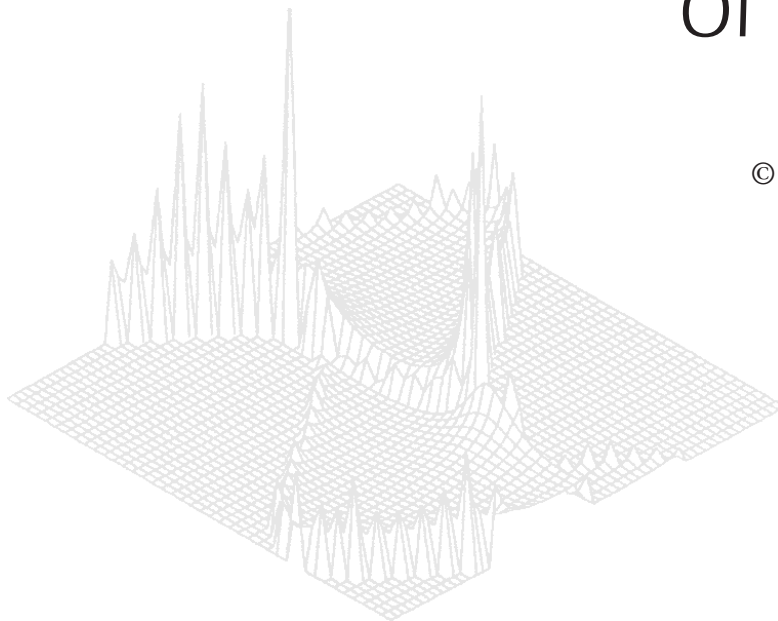

C S I R O P U B L I S H I N G

Australian Journal of Physics

Volume 52, 1999
© CSIRO Australia 1999



A journal for the publication of
original research in all branches of physics

www.publish.csiro.au/journals/ajp

All enquiries and manuscripts should be directed to

Australian Journal of Physics

CSIRO PUBLISHING

PO Box 1139 (150 Oxford St)

Collingwood

Vic. 3066

Australia

Telephone: 61 3 9662 7626

Facsimile: 61 3 9662 7611

Email: peter.robertson@publish.csiro.au



Published by **CSIRO PUBLISHING**
for CSIRO Australia and
the Australian Academy of Science



Helium Double Photoionisation and Compton Scattering: A Showcase for Electron Correlation*

U. Becker,^A G. Prümper,^A B. Langer,^A J. Viefhaus,^A M. Wiedenhöft,^A
J. C. Levin^B and I. A. Sellin^B

^AFritz-Haber-Institut der Max-Planck-Gesellschaft, Faradayweg 4–6,
D-14195 Berlin, Germany.

^BDepartment of Physics, University of Tennessee,
Knoxville, TN 37996–1200, USA.

Abstract

The present status of double photoionisation studies is comprehensively reviewed. Recent findings are described which shed some light on the transition from the correlated motion of the two electrons near threshold to the shakeoff-like behaviour at higher photon energies. For extremely high photon energies, where Compton scattering becomes the dominant process, new results for the $\text{He}^{2+}/\text{He}^+$ ratio between 6 and 120 keV are presented. The results confirm the prediction of Bergstrom *et al.* that the ratio reaches an intermediate maximum between 12 and 15 keV, before declining towards the asymptotic limit. Furthermore, this asymptotic limit seems not to be reached even at energies as high as 120 keV.

Many properties of gaseous and solid matter are well described within the framework of the independent particle model; the electron correlation may be neglected. The simplest system for studying the importance and specific behaviour of the electron correlation is atomic helium, where double photoexcitation and photoionisation are solely due to this phenomenon. Studies of the double excitation series (Domke *et al.* 1991, 1992; Madden and Codling 1963, 1965), photoelectron satellite intensities (Menzel *et al.* 1995) and angular distributions (Wehlitz *et al.* 1993) have led to the conclusion that the radial and angular electron parts of the wave function are well described within a molecular picture with different modes of vibrations (Herrick and Sinanoglu 1975; Kellmann and Herrick 1980). A fixed position of the two electrons with respect to each other is expected also to persist above the ionisation threshold and determine the near-threshold behaviour.

In order to study the two-electron emission behaviour above threshold, angle-resolved coincidence experiments are required either between the two electrons or the electron and the recoil ion. The first experiments in this respect were performed with the electron–electron coincidence technique. Schwarzkopf *et al.* (1993) measured the first angular pattern of electrons detected in coincidence with a second electron emitted in a fixed direction in a double photoionisation event. This angular pattern consisted basically of two lobes with characteristic

* Refereed paper based on a contribution to the Australia–Germany Workshop on Electron Correlations held in Fremantle, Western Australia, on 1–6 October 1998.

nodal structures. Maulbetsch and Briggs (1993*a*, 1993*b*) were the first to explain these characteristic features by symmetry considerations. The specific appearance of the angular patterns critically depends on the way in which the two electrons share the excess energy of the double ionisation. One distinguished mode is the equal energy sharing: the situation in which both electrons have exactly the same kinetic energy. In this case the two electrons become indistinguishable and particular symmetry rules have to be applied.

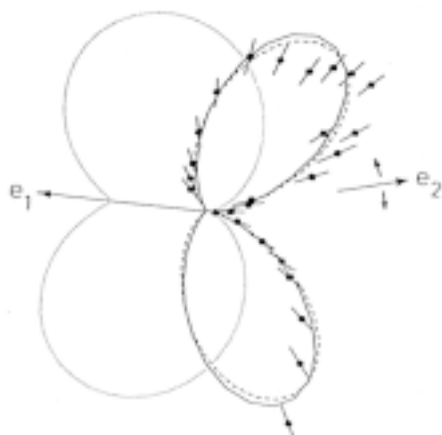


Fig. 1. Relative values of the experimental and theoretical triple-differential cross section (TDCS) for the double photoionisation of helium at $h\nu = 99$ eV in the plane perpendicular to the photon beam: the direction of the electron e_1 is fixed, while the electron e_2 is at different angles. For further details see Schwarzkopf *et al.* (1993).

Fig. 1 shows the first angular pattern measured with equal energy sharing (Schwarzkopf *et al.* 1993), and one can see that there are two nodes in the direction of the electric vector of the ionising electromagnetic radiation occurring either when the two electrons are emitted parallel or counter-parallel to each other: a situation also referred to as back-to-back emission. The parallel emission node is due to the Coulomb repulsion, which the two electrons experience when they start to escape. This forbidden parallel emission node is forced, for example, by the Sommerfeld factor in the two-electron wave function. The counter-parallel emission node, on the other hand, is the direct result of the symmetry laws governing the behaviour of two indistinguishable particles that obey Fermi statistics. Since the two electrons are in a 1P state their spin function is antisymmetric. In order to guarantee the antisymmetry of the total wave function, the space function has to be symmetric, which means that back-to-back emission is suppressed. This symmetry argument is only valid for the equal energy sharing case because in all other cases they become distinguishable, and therefore the strict validity of the symmetry law no longer holds. Essentially, already a small deviation from the equal sharing condition could result in a total breakdown of the nodal condition. This, however, does not happen.

The transition from the vanishing intensity for back-to-back emission at equal energy sharing to a noticeable intensity of unequal sharing is very smooth. This has been shown in an experiment in which the time-of-flight coincidence technique was used to measure the intensity distribution over kinetic energy sharing (see Fig. 2). This technique allows a simultaneous detection of all pairs of electrons with various kinetic energies. The experiment was carried out by Viehhaus *et al.* (1996) who demonstrated that it is possible to employ the time-of-flight

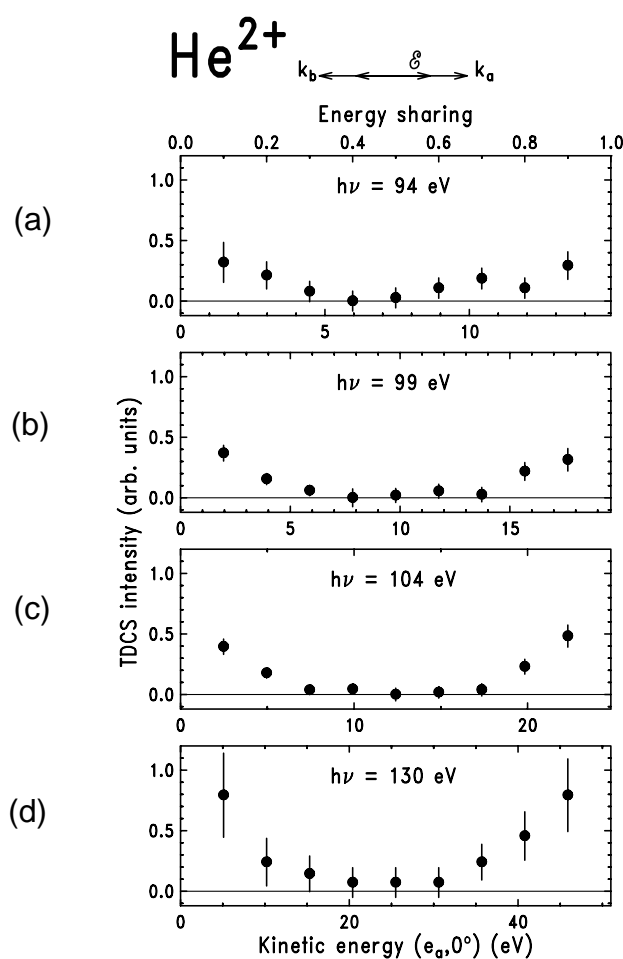


Fig. 2. TDCS for the double ionisation of He versus the kinetic energy E_1 of one of the two electrons measured at photon energies of (a) 94, (b) 99, (c) 104 and (d) 130 eV respectively. The emission directions are along the the direction of the linear polarisation axis at a relative angle θ_{12} of 180° .

technique for coincidence experiments and showed the above-mentioned transition for the first time. Furthermore, it proved that at higher excess energy and extremely unequal energy sharing the intensity in back-to-back emission reaches its maximum compared to all other directions. This has been obtained independently by Lablanquie *et al.* (1995) and could be reproduced by the calculations of Maulbetsch and Briggs (see Schwarzkopf *et al.* 1994) and Pont and Shakeshaft (1995). The question of what happens to the Coulomb node, i.e. to the parallel emission intensity when the energy sharing becomes ever more unequal, remains unanswered. In a way this question is related to the change in the overall shape of the angular pattern with energy sharing and excess energy.

Two experiments have shown (Dawber *et al.* 1995; Lablanquie *et al.* 1995) that the pattern change with energy sharing disappears at low excess energy, i.e. near threshold. In this case, the two lobe structure with two nodal points along the direction of the electric vector basically remains the same for all energy sharing conditions. On the other hand, it has been clearly proven that this situation changes dramatically at higher excess energies as outlined above. Malegat *et al.* (1997) have introduced a parametrisation of the triple differential cross section in terms of a gerade and ungerade transition amplitude:

$$\begin{aligned} \text{TDCS}(E_a, \theta_a, \theta_b) &= |a_g(E_a, E_b, \theta_{ab})(\cos\theta_a + \cos\theta_b) \\ &\quad + a_u(E_a, E_b, \theta_{ab})(\cos\theta_a - \cos\theta_b)|^2 \\ &\approx a_g^2 + a_u^2 + 2a_g a_u. \end{aligned}$$

These two amplitudes describe the different behaviour observed in the angular patterns with respect to the energy sharing and total excess energy. This parametrisation offers the opportunity to separate the different contributions and possibly find an explanation for the angular pattern variation from near-threshold to higher excess energies. In order to explore the potential of this parametrisation for the interpretation of the double photoionisation of helium, we have analysed a series of older data along with new angular patterns at $h\nu = 99$ eV in terms

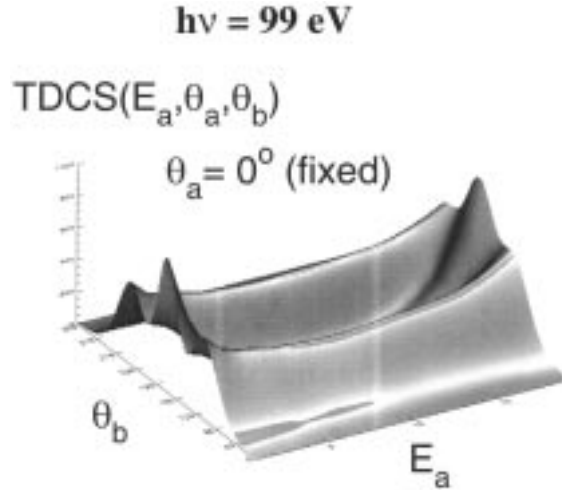


Fig. 3. Three-dimensional representation of the TDCS over the kinetic energy E_a of electron a and emission angle θ_b of electron b . The emission angle θ_b is fixed along the electric vector of the ionising radiation (Wiedenhöft *et al.* 1998).

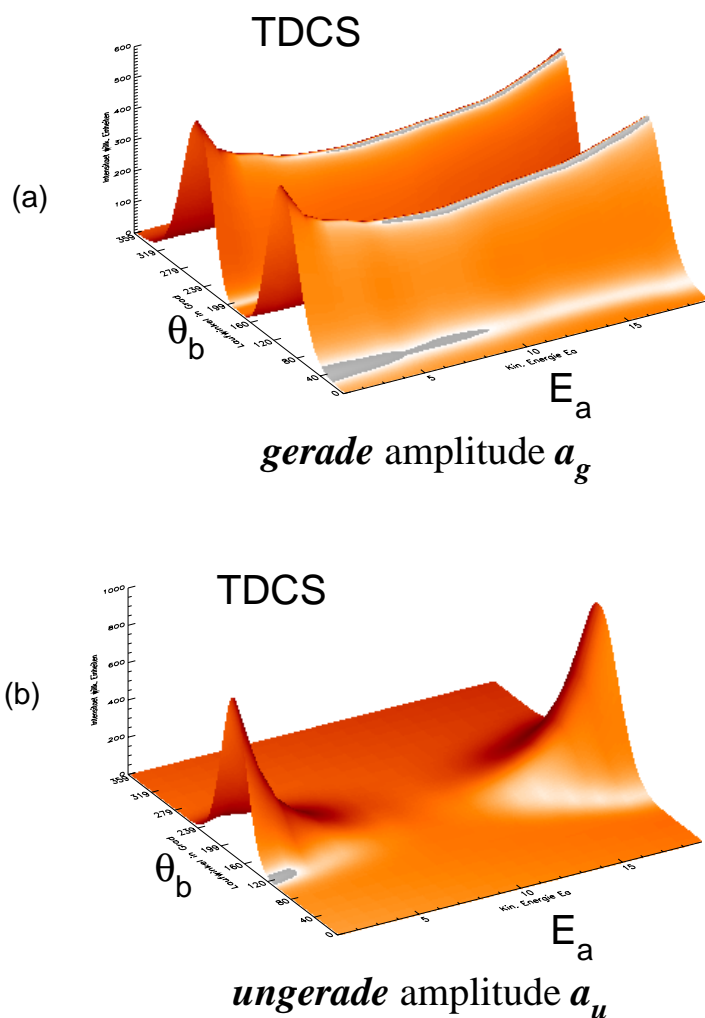


Fig. 4. Separate representation of (a) the gerade and (b) the ungerade part of the TDCS in Fig. 3 (Wiedenhöft *et al.* 1998).

of the gerade and ungerade amplitude. The details of this analysis as well as the measurements will be published elsewhere. Here we just want to show a two-dimensional representation of the fitted results.

Fig. 3 shows the triple differential cross section (TDCS) over the kinetic energy E_a and the emission angle θ_b of electron b with respect to the electric vector E for θ_a fixed at 0° . We note that the ungerade amplitude has a remarkable intensity under extreme energy sharing conditions and back-to-back emission ($\theta_b \geq 180^\circ$) only. The two amplitudes are shown separately in Fig. 4. It is evident that the gerade amplitude shows little variation over the kinetic energy. The two-dimensional intensity distribution reflects the two lobe patterns independent of energy sharing which has been observed near

threshold. This confirms the conclusion of Lablanquie *et al.* (1995) that the gerade amplitude is the dominant part in near-threshold double photoionisation. The ungerade amplitude, on the other hand, shows strong energy dependence in accordance with the findings of Viehaus *et al.* (1996) shown in Fig. 2. These two intensity plots make it clear that the Coulomb repulsion node for parallel emission is not only enforced in equal energy sharing but also gives rise to a vanishing intensity over a wide range of kinetic energies. This is in contrast to the behaviour of the symmetry node in back-to-back emission, which completely loses relevance at extreme energy sharing; in this case maximal intensity is emitted along this direction. In order to visualise these results, it is useful to transform the electron–electron coincidence patterns into recoil-ion electron-pair emission patterns.

For the first time, such patterns have been measured by Dörner *et al.* (1996) using recoil-ion momentum spectroscopy. In this experiment they showed the recoil ion momentum distribution of the He^{2+} which is the negative momentum distribution of the two electrons. This distribution has its peak preferentially along the direction of the electric vector. Knowing that the two electrons are moving together along the electric vector, the question arises as to what their relative momentum distribution is, or—in other words—how they move in their centre-of-mass system. The results of Dörner *et al.* nicely showed that the two electrons move preferentially back-to-back in a direction perpendicular to the electric vector, thus confirming the prediction of the Wannier theory for near-threshold double photoionisation. On the other hand, it is known from non-coincident angular distribution measurements of electrons emitted during double photoionisation of helium at higher photon energies that the fast electron is ejected preferentially along the electric vector direction. The question arises as to how this transition to a completely different behaviour actually occurs. Does the correlated motion of the two electrons exhibited near threshold change its character or is it simply losing relative strength with respect to what one might consider an uncorrelated motion or shakeoff behaviour? In this case one would expect that at intermediate energies both kinds of behaviour occur, although possibly with rather different strengths. In order to prove this assumption, we have transformed the electron–electron coincidence distributions shown in Figs 3 and 4 into recoil-ion momentum distributions and relative electron–electron distributions (see Fig. 5). When we take the total momentum distributions shown in Fig. 3, we obtain a relative electron momentum distribution very similar to the one observed by Dörner *et al.* using recoil-ion momentum spectroscopy. When we go further, however, we find a very interesting and unexpected result: the sum distribution splits into two separate distributions which are orthogonal to each other with respect to their preferential emission direction. Whereas the gerade amplitude corresponds to a ‘correlated’ Wannier case with electron motion in the centre-of-mass system perpendicular to the electron vector, the ungerade amplitude gives rise to a preferred electron motion along this vector. This momentum distribution comes from electrons with very unequal energy sharing. Since this sharing situation becomes more and more dominant at higher photon energies this emission mode also becomes dominant. It is still an open question if there remains a small background of ‘correlated electrons’ in the sense of the gerade amplitude. Similar studies at higher photon energies where unequal energy sharing dominates are required.

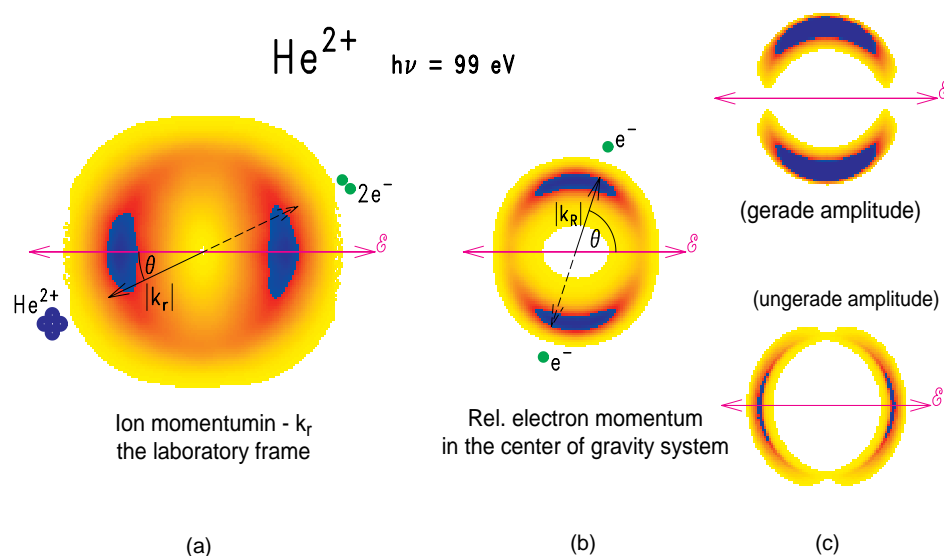


Fig. 5. (a) Recoil ion momentum distribution and (b) the relative electron–electron momentum distribution in the centre of gravity frame of the two electrons. Part (c) again shows the separation of (b) into the gerade and ungerade part of the transition amplitude.

In this limit, photoionisation loses importance compared to Compton scattering which, on the other hand, gains importance with increasing photon energy; both processes are of equal strength around 6 keV. An interesting problem in this context is the existence of an intermediate maximum in the $\text{He}^{2+}/\text{He}^+$ ratio above 10 keV before this ratio starts to decline to the asymptotic limit of 0.83%. The data points in this region are very scarce and do not allow a definite conclusion to be drawn on whether this maximum exists at all and what is its absolute height. Similarly unclear is the situation at the asymptotic limit. In order to prove the theoretical prediction of this limit, Wehlitz *et al.* (1996) in a first step have measured the ratio between doubly and singly charged ions produced by Compton scattering at an energy of 57 keV in the hard X-ray regime. They derived a value well above the asymptotic limit Spielberger *et al.* (1996) measured the same ratio and obtained a lower result which was relatively close to the predicted asymptotic limit values of 0.80% to 0.84%, depending on the calculation.

In this paper we report on new and extended measurements of the $\text{He}^{2+}/\text{He}^+$ ratio regarding the intermediate maximum and the value of the asymptotic limit. Two sets of measurements were performed, one at the National Synchrotron Light Source (NSLS) beamline X25, and the other one at the European Synchrotron Radiation Facility (ESRF) beamline ID15. In the first set of measurements, the experimental setup was the same as in former experiments (Levin *et al.* 1996; Wehlitz *et al.* 1996) and in the second set a different ion spectrometer was used. Figs 6a and 6b show two ion yield spectra taken at 66 keV and 120 keV respectively. The $\text{He}^{2+}/\text{He}^+$ ratios obtained from both sets of measurements are shown in Fig. 7, together with the former measurements and other new and still

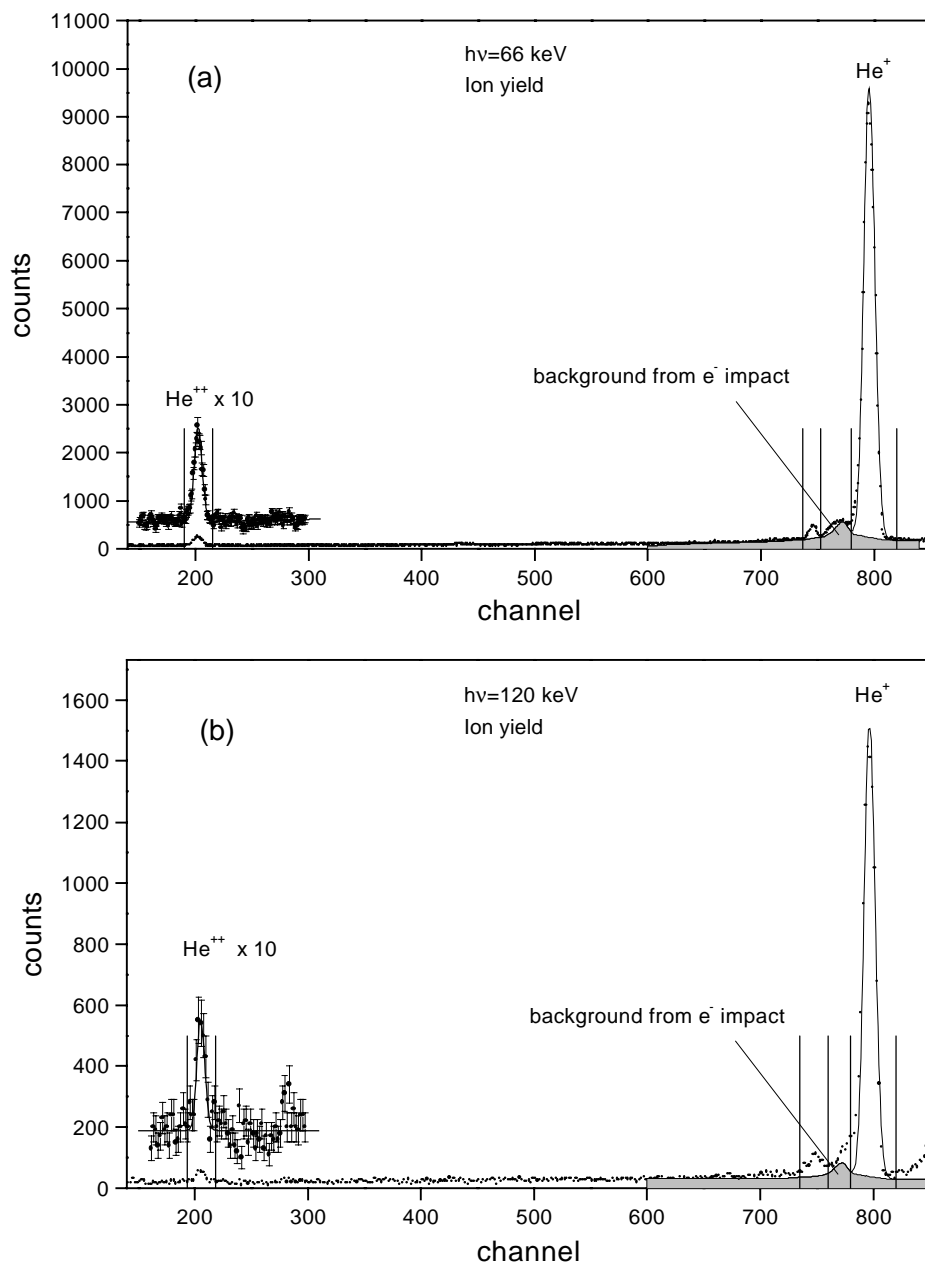


Fig. 6. Ion yield spectra taken at (a) 66 keV and (b) 120 keV.

unpublished data. The results between 6 and 11 keV confirm very nicely the upward trend to the intermediate maximum predicted by Bergstrom *et al.* There is no doubt that the $\text{He}^{2+}/\text{He}^+$ ratio increases at least 14% above 6 keV to the local maximum between 11 and 15 keV before declining to the asymptotic limit. For this limit there are now more points available than for the two measurements

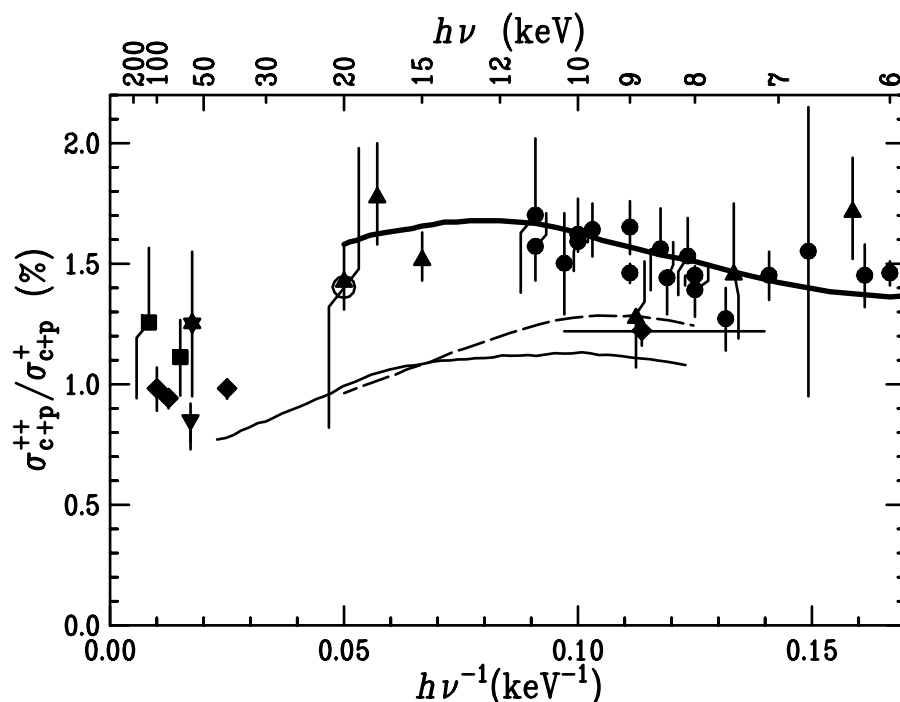


Fig. 7. Helium double-to-single ionisation ratio shown as function of the reciprocal photon energy. Individual symbols represent experimental data: present results (squares: ERSF, closed circles: NLS) and previous results: triangles (Levin *et al.* 1996), star (Wehlitz *et al.* 1996), diamonds (Spielberger *et al.* 1995), inverted triangle (Spielberger *et al.* 1999) and open circle (Samson *et al.* 1996). The curves represent the theoretical calculations: thin solid (Andersson and Burgdörfer 1993); dashed, uncorrelated final state (Andersson and Burgdörfer 1994); bold solid, Compton and photoionisation (Bergstrom *et al.* 1995).

at 57 keV by Wehlitz *et al.* and Spielberger *et al.* The data known at present cover an energy range between 40 and 120 keV, a range wide enough to decide whether the asymptotic limit has already been reached or not.

There are still relatively great uncertainties in some data points, and the different sets of measurements deviate from each other, but the present data set seems to converge to 1.0 ± 0.1 if one takes all data sets together weighted by their given error bars. This is well above most of the theoretical predictions for the asymptotic limit showing that there is still ambiguity concerning the transition from the intermediate energy measurements to the asymptotic limit. The present data lead to the conclusion that this limit may be reached much more smoothly over a very wide energy range than expected from different theoretical predictions (Anderson and Burgdörfer 1993, 1994; Bergstrom *et al.* 1995; Hino *et al.* 1994; Suric *et al.* 1994). In order to compare the pure Compton data over a logarithmic energy scale we have extracted them from the combined photoionisation and Compton data, using the relative ratio between the two processes as given by Bergstrom *et al.* (1995) (see Fig. 8). This separation yields different values only for σ_c below 9 keV, for all data points above this energy the $\text{He}^{2+}/\text{He}^+$ values shown in Fig. 8 are the same as in Fig. 7. The theoretical

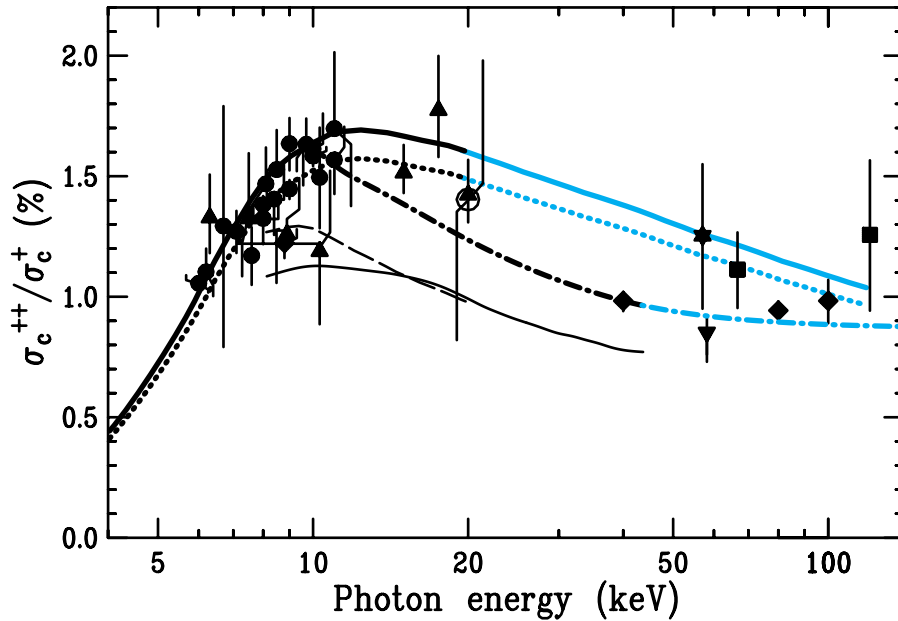


Fig. 8. Helium Compton double-to-single ionisation ratio shown as function of the photon energy. Individual symbols represent experimental data: present results (squares: ERSF, closed circles: NLS) and previous results: triangles (Levin *et al.* 1996), star (Wehlitz *et al.* 1996), diamonds (Spielberger *et al.* 1995), inverted triangle (Spielberger *et al.* 1999) and open circle (Samson *et al.* 1996). Our NLS data (circles) and the values from Levin *et al.* (1996) are calculated from the respective values shown in Fig. 7 by multiplying with a correction function as described in the text. The curves represent the theoretical calculations: thin solid (Andersson and Burgdörfer 1993); dashed, uncorrelated final state (Andersson and Burgdörfer 1994); bold solid, Compton only (Bergstrom *et al.* 1995). The grey solid curve shows a linear extrapolation (in logarithmic scale) of the latter theoretical curve. The dotted curve is obtained from Bergstrom *et al.* (1995) and its extrapolation by multiplying by 0.93 in order to adjust it to the bulk of the experimental data. Similarly, the dash-dot curve was obtained from the Andersson curve multiplied by 1.17.

curves of Andersson and Burgdörfer (1993, 1994) and Bergstrom *et al.* (1995) were adjusted to the bulk of the low and intermediate energy data in order to compare their extrapolated curvature towards the asymptotic limit with the present experimental data at high energy. This representation shows that there is still a gap of data points between 20 and 40 keV to be closed before definite conclusions can be drawn on how the asymptotic limit is actually approached.

Summarising one can say that our understanding of the double photoionisation of helium has made tremendous progress during the last years. We are now able to understand the correlated motion of the two emitted electrons near threshold but also at intermediate energies. At very high energies the intermediate maximum and the transition to the asymptotic limit of the $\text{He}^{2+}/\text{He}^+$ ratio due to Compton scattering are now also reasonably well documented, although not totally understood in every detail. These results along with former measurements will certainly trigger new theoretical calculations in order to understand the transition to the asymptotic limit in a more quantitative way.

Acknowledgments

The authors are indebted to the Deutsche Forschungsgemeinschaft for financial support. They are most grateful to Th. Tschentscher and Th. Buslaps at the ESRF beamline.

References

- Andersson, L. R., and Burgdörfer, J. (1993). *Phys. Rev. Lett.* **71**, 50.
- Andersson, L. R., and Burgdörfer, J. (1994). *Phys. Rev. A* **50**, R2810.
- Bergstrom, P. M., Hino, K., and Macek, J. H. (1995). *Phys. Rev. A* **51**, 3044.
- Dawber, G., Avaldi, L., McConkey, A. G., Rojas, H., MacDonald, M. A., and King, G. C. (1995). *J. Phys. B* **28**, L271.
- Domke, M., Puschmann, C. X. A., Mandel, T., Hudson, E., Shirley, D. A., Kaindl, G., Greene, C. H., Sadeghpour, H. R., and Peterson, H. (1991). *Phys. Rev. Lett.* **66**, 1306.
- Domke, M., Remmers, G., and Kaindl, G. (1992). *Phys. Rev. Lett.* **69**, 1171.
- Dörner, R., Feagin, J. M., Cocke, C. L., Bräuning, H., Jagutzki, O., Jung, M., Kanter, E. P., Khemliche, H., Kravis, S., Mergel, V., Prior, M. H., Schmidt-Böcking, H., Spielberger, L., Ullrich, J., Unversagt, M., and Vogt, T. (1996). *Phys. Rev. Lett.* **77**, 1024.
- Herrick, D. R., and Sinanoglu, O. (1975). *Phys. Rev. A* **11**, 97.
- Hino, K., Bergstrom, P. M., and Macek, J. H. (1994). *Phys. Rev. Lett.* **72**, 1620.
- Kellmann, M. E., and Herrick, D. R. (1980). *Phys. Rev. A* **22**, 1536.
- Lablanquie, P., Mazeau, J., Andric, L., Selles, P., and Huetz, A. (1995). *Phys. Rev. Lett.* **74**, 2192.
- Levin, J. C., Armen, G. B., and Sellin, I. A. (1996). *Phys. Rev. Lett.* **76**, 1220.
- Madden, R. P., and Codling, K. (1963). *Phys. Rev. Lett.* **10**, 516.
- Madden, R. P., and Codling, K. (1965). *Astrophys. J.* **141**, 364.
- Malegat, L., Selles, P., and Huetz, A. (1997). *J. Phys. B* **30**, 251.
- Maulbetsch, F., and Briggs, J. S. (1993a). *J. Phys. B* **26**, 1679.
- Maulbetsch, F., and Briggs, J. S. (1993b). *J. Phys. B* **26**, L647.
- Menzel, A., Frigo, S., Whitfield, S. B., Caldwell, C. D., Krause, M. O., Tang, J. Z., and Shimamura, I. (1995). *Phys. Rev. Lett.* **75**, 1479.
- Pont, M., and Shakeshaft, R. (1995). *Phys. Rev. A* **51**, R2676.
- Samson, J. A. R., He, Z. X., Stolte, W., and Cutler, J. N. (1996). *J. Elect. Spectrosc. Relat. Phenom.* **78**, 19.
- Schwarzkopf, O., Krässig, B., Elmiger, J., and Schmidt, V. (1993). *Phys. Rev. Lett.* **70**, 3008.
- Schwarzkopf, O., Krässig, B., Schmidt, V., Maulbetsch, F., and Briggs, J. S. (1994). *J. Phys. B* **27**, L345.
- Spielberger, L., Jagutzki, O., Dörner, R., Ullrich, J., Meyer, U., Mergel, V., Unversagt, M., Damrau, M., Vogt, T., Ali, I., Khayyat, K., Bahr, D., Schmidt, H. G., Frahm, R., and Schmidt-Böcking, H. (1995). *Phys. Rev. Lett.* **74**, 4615.
- Spielberger, L., Jagutzki, O., Krässig, B., Meyer, U., Khayyat, K., Mergel, V., Tschentscher, T., Buslaps, T., Bräuning, H., Dörner, R., Vogt, T., Achler, M., Ullrich, J., Gemmel, D. S., and Schmidt-Böcking, H. (1996). *Phys. Rev. Lett.* **76**, 4685.
- Spielberger, L., Bräuning, H., Muthig, A., Tang, J. Z., Wang, J., Qiu, Y., Dörner, R., Jagutzki, O., Tschentscher, T., Honkimäki, V., Mergel, V., Achler, M., Weber, T., Khayyat, K., Burgdörfer, J., McGuire, J., and Schmidt-Böcking, H. (1999). *Phys. Rev. A* **59**, 371.
- Suric, T., Pisk, K., Logan, B., and Pratt, R. (1994). *Phys. Rev. Lett.* **73**, 790.
- Viefhaus, J., Avaldi, L., Heiser, F., Hentges, R., Gessner, O., Rüdell, A., Wiedenhöft, M., Wieliczek, K., and Becker, U. (1996). *J. Phys. B* **29**, L729.
- Wehlitz, R., Hentges, R., Prümper, G., Farhat, A., Buslaps, T., Berrah, N., Levin, J. C., Sellin, I. A., and Becker, U. (1996). *Phys. Rev. A* **53**, R3720.
- Wehlitz, R., Langer, B., Berrah, N., Whitfield, S. B., Viefhaus, J., and Becker, U. (1993). *J. Phys. B* **26**, L783.
- Wiedenhöft, M., Viefhaus, J., Heiser, F., Hentges, R., Hempelmann, A., and Becker, U. (1998). Twelfth Int. Conf. on Vacuum Ultraviolet Radiation Physics, Program and Abstracts, Th004.